

# Experimental observation of near-motion-trapped mode

H. Wolgamot<sup>1</sup>, P. H. Taylor<sup>2</sup>, R. Eatock Taylor<sup>2</sup>, C.J. Fitzgerald<sup>2</sup>,  
T. van den Bremer<sup>2</sup>, C. Whittaker<sup>3</sup>, A. Raby<sup>3</sup>

<sup>1</sup> Faculty of Engineering, Computing and Mathematics, University of Western Australia  
35 Stirling Highway, CRAWLEY WA 6009, Australia. hugh.wolgamot@uwa.edu.au

<sup>2</sup> Department of Engineering Science, University of Oxford, OX1 3PJ, UK

<sup>3</sup> School of Marine Science and Engineering, Plymouth University, PL4 8AA, UK

## Highlights

- Near-motion-trapping in heave is demonstrated experimentally;
- Tuned and detuned geometries tested;
- Range of radiation damping values is apparent from body motion;
- Small differences in damping apparent in analysis of radiated field.

## 1 Introduction

Trapped modes and near-trapped modes have been of considerable interest in water-wave problems for some time; sloshing trapped modes around fixed structures were found by Callan et al. [1991] and many subsequent authors, while sloshing near-trapped modes were found in arrays of vertical circular cylinders by Evans and Porter [1997]. Motion-trapped modes, in which a structure moves with a local oscillation of the free surface, but no oscillation in the far-field, were discovered by McIver and McIver [2006]. A previous contribution to this workshop, subsequently published as Wolgamot et al. [2014], identified a structure which approximated motion-trapping characteristics to high accuracy: 8 heaving truncated circular cylinders, evenly spaced around the circumference of a circle. The theoretical investigations above (and other similar works) have used potential flow theory.

Experimental investigations of sloshing trapped modes were undertaken by Cobelli et al. [2011], while various authors have investigated sloshing near-trapped modes experimentally. However, no

attempt has been made to investigate motion-trapped (or near-trapped) modes experimentally to the authors' knowledge. Hence this paper describes a small experimental campaign to investigate the 8 cylinder structure referred to above.

## 2 Experimental methods

As the theory of motion-trapped modes assumes an ideal fluid it was desirable to minimise viscous effects in the experiments. To this end, the 8 cylinder structure investigated had hemispherical ends on each cylinder - the predicted trapping behaviour was not significantly altered compared to the truncated cylinders, though the trapping frequency changed as a result of the change in added mass. Each cylinder was fabricated from 160mm dia. PVC pipe, with a (clear) plastic hemisphere of the same diameter attached to the bottom. The cylinders were attached by radial spokes to a central hub, and could be attached at different positions along the spokes to change the radius of the ring, while adjusting the ballast in the cylinders adjusted the draft. Water was used as ballast - no internal sloshing was observed so there was no need to attempt to suppress such oscillations.

Tests were carried out in the Coastal Basin at Plymouth University's COAST Laboratory. This facility is a rectangular basin 15.5m x 10m, with an array of piston-type wavemakers (switched off throughout testing) and a beach on opposite short sides and 0.5m water depth during testing. The model was suspended from a beam across the tank (with the hemispherical ends completely immersed in all cases) and then released using a latch system. The motion of the model was tracked using a 6 DOF motion tracking system and the motion

of the free surface measured by wave gauges at seven points (both systems sampling at 128 Hz). The wave gauge locations are shown in Figure 1; Figure 2 is a photo of the experimental set-up.

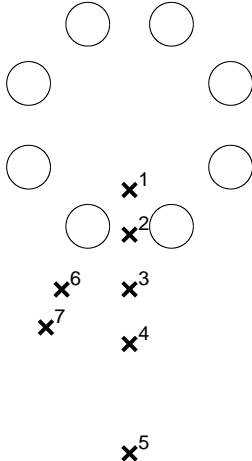


Figure 1: Layout of wave gauges WG1-WG7 (indicated by numbered crosses) relative to the cylinders for ring radius  $5a$ . Note that the wave gauges were not moved when the ring radius was changed.

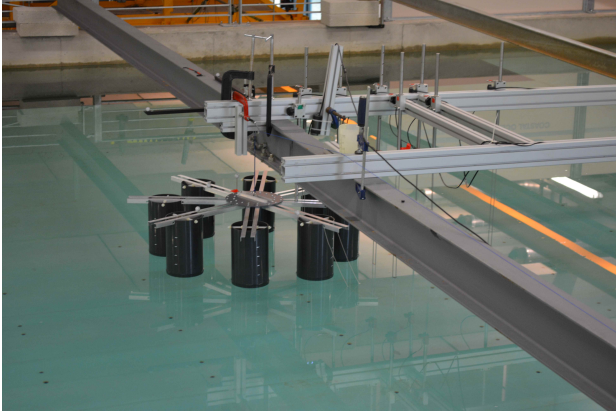


Figure 2: Experimental set-up showing model and wave gauges attached to the support beams.

The near-motion-trapped geometry had a ring radius of  $5a$ , where  $a$  is the cylinder radius, and an equilibrium draft of  $2.5a$ . In addition to this tuned case, a number of de-tuned cases, with different ring radii and drafts, were tested in the same way. The test geometry matrix is given in Table 1.

### 3 Results

One problem affecting both body motion and wave gauge data is reflection from the sidewalls of the tank. Based on the wave gauge readings it is estimated that the reflected waves from the sidewall reached the model about 5 seconds after release.

Draft \ Radius	$4a$	$5a$	$6a$
$2a$		$0.5a$	
$2.5a$	$0.5a$	$0.5a$	$0.5a$
	$0.75a$	$0.75a$	$0.75a$
	$a$	$a$	$a$
$3a$		$0.5a$	
		$0.75a$	
		$a$	
$3.5a$	$0.5a$	$0.5a$	
	$0.75a$	$0.75a$	

Table 1: Test matrix of different 8 cylinder configurations tested. Entries of the table correspond to initial release height. The near-motion-trapped mode occurs at draft  $2.5a$  and ring radius  $5a$ .

#### 3.1 Model heave

The model heave motion was found to behave linearly - no higher harmonics were evident when the frequency content was examined and the time series for different release heights, scaled by the initial value, matched extremely well (as seen in Figure 3). This behaviour suggests that nonlinear viscous damping of the model was negligible and that the viscous damping present can be considered linear. The different geometries were predicted to exhibit a range of radiation damping values - as indicated in Table 2.

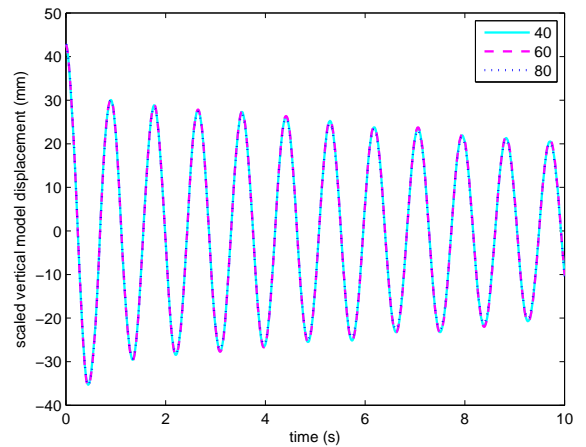


Figure 3: Heave oscillations of model at three different release heights, normalised by initial release height (to match nominal 40mm, actual release 43mm) to indicate linear scaling.

A number of methods were used to investigate the damping of the model. Dramatically different behaviour was observed for the most and least damped cases, as shown in Figure 4. However, it was difficult to differentiate between the decay

Draft	Radius	4a	5a	6a
2a			2.7	
2.5a		1.9	0.0018*	0.9
3a			3.0	
3.5a		29	10	

Table 2: Predicted linear radiation damping of the various geometries tested (kg/s). \*Note that this geometry is still slightly mistuned - at a frequency  $\simeq 0.002$  Hz higher the predicted damping is more than 2 orders of magnitude lower, though this has little relevance experimentally.

rates of the models with small radiation damping, where the differences were masked by viscous damping. No simple theoretical way of accurately calculating the viscous damping to eliminate it from the problem could be found, but further analysis will be reported at the workshop. Figure 5 illustrates the behaviour of the different models by means of a plot of the predicted and measured natural periods and damping coefficients for each of the geometries given in Table 2. The damping is shown on a log scale. Note also in this figure the generally good agreement between predicted and measured oscillation period.

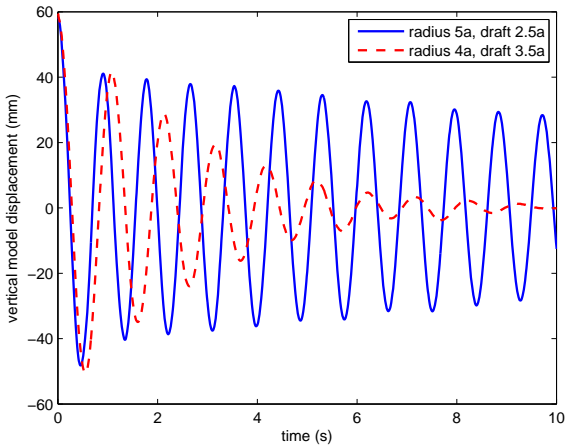


Figure 4: Measured time series of model oscillations in heave for the tuned geometry and geometry with the highest radiation damping.

### 3.2 Free surface elevation

The free surface elevation data was filtered in the frequency domain to remove the signal due to vibrations of the supporting beam (which supported both the model and wave gauges). As this beam vibration frequency occurred at approximately 5.5Hz, much higher than the wave fre-

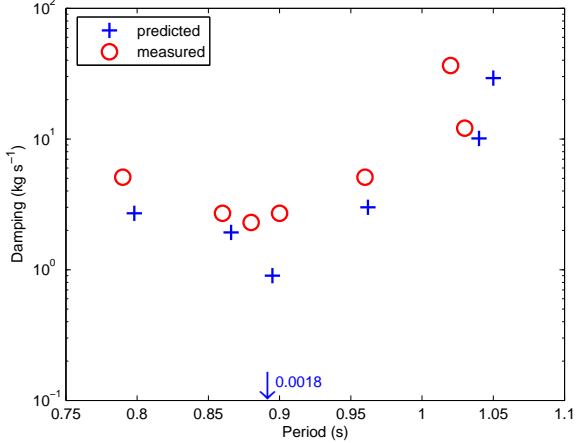


Figure 5: Predicted and measured model oscillation period and damping. The arrow indicates the predicted values for the tuned case (third from left).

quencies, this was straightforward. In contrast to the model heave data, and as expected, higher harmonics were found to be present in the free surface elevation data. The radiated field data distinguished between the near-motion-trapped case and the other cases with moderately low damping. This is shown in Figure 6, where the time series and the Fourier transformed data (calculated using  $2^{12}$  points, i.e. 32 seconds, commencing at 1.5 seconds after release) are shown for the near-motion-trapping geometry and the geometry with the 2nd lowest radiation damping (ring radius 6a, draft 2.5a).

Figure 6a shows the time series of the free surface elevations for the tuned case. It may be seen that in the tuned case, after the initial transient has passed, there is negligible radiation at linear frequencies outside the array (WG3) despite the fact that the internal free surface continues to oscillate. A comparison of the power spectral density at the heave frequency for wave gauges 1 and 3 (inside and outside the array) shows a ratio of almost  $10^3$  for the optimised geometry. There is noticeable radiation at double the linear frequency and the arrival of reflections at about 5 seconds may be seen. Figure 6b shows this pronounced 2nd harmonic and the absence of a linear signal outside the array. In Figures 6c and 6d, by contrast, there is a clear linear signal outside the array which dominates over the 2nd harmonic. It should be noted that the relative position of WG3 is closer to the model when the ring radius is increased, but as WG4 to 7 (omitted here for clarity) show similar behaviour this point is not significant.

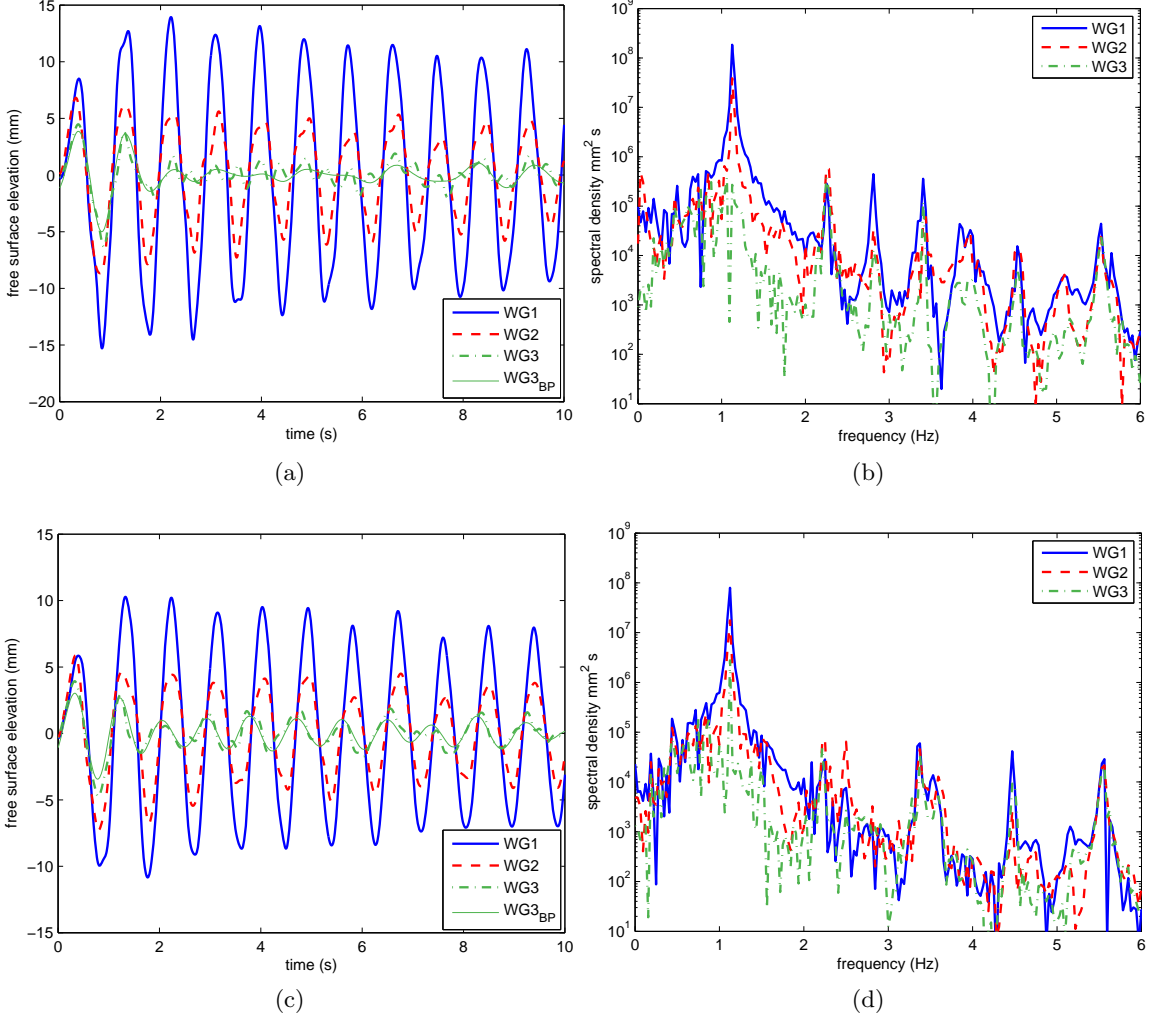


Figure 6: (a) time series of free surface elevations for the tuned case (ring radius  $5a$ , draft  $2.5a$ ). WG3<sub>BP</sub> is band pass filtered to eliminate frequencies outside the range  $0.5f_1 < f < 1.5f_1$ , where  $f_1$  = peak linear frequency; (b) power spectrum for case (a); (c) time series for ring radius  $6a$ , draft  $2.5a$ ; (d) power spectrum for case (c).

## 4 Conclusions

Even though viscous damping is present in the experiments, the behaviour of the near-trapped mode is retained and is clearly visible: the heave motion persists for longer, and there is little wave radiation at the heave frequency after a starting transient. Further analysis, including fully nonlinear simulations of the experiment and videos taken during the testing will be presented at the Workshop.

## Acknowledgement

The authors are grateful to the Lubbock Trustees in Oxford for a small grant to cover the costs of construction of the model. The first author acknowledges financial support from Shell Australia.

## References

- M. Callan, C.M. Linton, and D.V. Evans. Trapped modes in two-dimensional waveguides. *Journal of Fluid Mechanics*, 229:51–64, 1991.
- P.J. Cobelli, V. Pagneux, A. Maurel, and P. Petitjeans. Experimental study on water-wave trapped modes. *Journal of Fluid Mechanics*, 666:445–476, 2011.
- D.V. Evans and R. Porter. Near-trapping of waves by circular arrays of vertical cylinders. *Applied Ocean Research*, 19:83–99, 1997.
- P. McIver and M. McIver. Trapped modes in the water-wave problem for a freely floating structure. *Journal of Fluid Mechanics*, 558(1):53–67, 2006.
- H.A. Wolgamot, R. Eatock Taylor, and P.H. Taylor. Radiation, trapping and near-trapping in arrays of floating truncated cylinders. *Journal of Engineering Mathematics*, Published online 23 October 2014; DOI: 10.1007/s10665-014-9734-1, 2014.